Water-Soluble Pegylated Quantum Dots: From a Composite Hexagonal Phase to Isolated Micelles

F. Boulmedais,[†,▽] P. Bauchat,[†] M. J. Brienne,[‡] I. Arnal,[§] F. Artzner,[||] T. Gacoin,[⊥] M. Dahan,[#] and V. Marchi-Artzner*,[†]

Université de Rennes 1, Sciences Chimiques de Rennes, CNRS UMR 6226, Campus de Beaulieu, F-35042 Rennes Cedex, France, Chimie des Interactions Moléculaires, CNRS UPR 285, 11 place Marcelin Berthelot, F-75005 Paris, Université de Rennes 1, Interactions Cellulaires et Moléculaires, CNRS UMR 6026, Campus Beaulieu, F-35042 Rennes, Cedex France, Université de Rennes 1, Groupe Matière Condensée et Matériaux, CNRS UMR 6626, F-35042 Rennes Cedex, France, Laboratoire de Physique de la matière condensée, CNRS UMR 7643, Ecole Polytechnique, Route de Saclay, F-91128 Palaiseau Cedex, France, and Laboratoire Kastler Brossel, CNRS UMR 8552, Ecole Normale Supérieure et Université Pierre et Marie Curie, 24 rue Lhomond, F-75005 Paris, France

Received June 27, 2006. In Final Form: August 30, 2006

We present a simple method based on the dispersion of fluorescent quantum dots (QD) into a liquid crystal phase that provides either nanostructured material or isolated QD micelles depending on water concentration. The liquid-crystal phase was obtained by using a gallate amphiphile with a poly(ethylene glycol) chain as the polar headgroup, named **I**. The hydration of QD/**I** mixtures resulted in the formation of a composite hexagonal phase identified by small-angle X-ray scattering and by polarized light and fluorescence optical microscopy, showing a homogeneous distribution of fluorescence within hexagonal phase. This composite mesophase can be converted into isolated QD-**I** micelles by dilution in water. The fluorescent QD-**I** micelles, purified by size exclusion chromatography, are well monodisperse with a hydrodynamic diameter of 20−30 nm. Moreover, these QD do not show any nonspecific adsorption on lipid or cell membranes. By simply adjusting the water content, the PEG gallate amphiphile **I** provides a simple method to prepare a self-organized composite phase or pegylated water soluble QD micelles for biological applications.

Introduction

Due to their well-controlled nanometer size and their unique luminescent properties[1,2] semiconductor colloidal quantum dots (QD) are of great interest, either as biological markers in vitro[3,4] and in vivo[5] or as building blocks for nanostructured materials with specific optical properties.[6,7] Using QD in these two fields of applications usually involves their surface modifications and requires satisfying very different conditions. For biolabeling, the goal is to prepare monodisperse functionalized nanoparticles whereas for nanomaterials, the main effort is to organize nanocrystals into a condensed and ordered state. Unsurprisingly, these almost opposite requirements have led to distinct chemical approaches. On one hand, many chemical methods have been developed to water-solubilize QD for their use as nanoprobes in biological systems. In the familiar case of CdSe/ZnS particles stabilized by a hydrophobic trioctylphosphine oxyde (TOPO) ligand,[8,9] a successful approach is based on the surface−ligand exchange, in which TOPO molecules are replaced with bifunctional molecules, such as cysteines,[10] mercapto alkanoic acids,[11,12] or oligomeric phosphines.[13] Another fruitful approach consists of encapsulating QD with an amphiphilic monolayer of phospholipids,[3,14] polymers,[5,15−17] or more recently calixarene derivatives,[18] thanks to hydrophobic interactions between TOPO and the hydrophobic part of the amphiphile.

On the other hand, self-assembled molecular systems have been successfully used as templates for the nucleation of nanocrystals and thus for the preparation of well-defined ordered materials. Soft biomaterials, such as bacteriophage viruses presenting strong interaction for ZnS crystal surfaces, have been also successfully employed to prepare multi-length scale ordering of QD hybrid self-supporting structures.[19] ZnS and CdS nanocrystals were nucleated in a lyotropic liquid crystalline medium

* To whom correspondence should be addressed. Tel: +33 (0)2 23 23 62 72. Fax: +33 (0)2 23 23 67 38. E-mail: valerie.marchi-artzner@univ-rennes1.fr.
[†] CNRS UMR 6226.
[‡] CNRS UPR 285.
[§] CNRS UMR 6026.
[||] CNRS UMR 6626.
[⊥] CNRS UMR 7643.
[#] CNRS UMR 8552.
[▽] Present address : Institut Charles Sadron, CNRS UPR22, 6 rue Boussingault, BP40016, F-67083 Strasbourg Cedex, France.

(1) Murray, C. B.; Norris, D. J.; Bawendi, M. G. *J. Am. Chem. Soc.* **1993**, *115*, 8706−8715.
(2) Alivisatos, A. P. *Science* **1996**, *271*, 933−937.
(3) Dubertret, B.; Skourides, P.; Norris, D. J.; Noireaux, V.; Brivanlou, A. H.; Libchaber, A. *Science* **2002**, *298*, 1759−1762.
(4) Dahan, M.; Levi, S.; Luccardini, C.; Rostaing, P.; Riveau, B.; Triller, A. *Science* **2003**, *302*, 442.
(5) Gao, X.; Cui, Y.; Levenson, R. M.; Chung, L. W. K.; Nie, S. *Nat. Biotechnol.* **2004**, *22*, 969−976.
(6) Douglas, T.; Young, M. *Nature* **1998**, *393*, 167.
(7) Braun, P. V.; Osenar, P.; Tohver, V.; Kennedy, S. B.; Stupp, S. I. *J. Am. Chem. Soc.* **1999**, *121*, 7302−7309.
(8) Hines, M. A.; Guyot-Sinnest, P. *J. Phys. Chem.* **1996**, *100*, 468.
(9) Dabboussi, B. O.; Rodriguez-Viejo, J.; Mikulec, F. V.; Heine, J. R.; Mattoussi, H.; Ober, R.; Jensen, K. F.; Bawendi, M. G. *J. Phys. Chem. B* **1997**, *101*, 9463−9475.
(10) Pinaud, F.; King, D.; Moore, H. P.; Weiss, S. *J. Am. Chem. Soc.* **2004**, *126*, 6115−6123.
(11) Chan, W. C.; Nie, S. *Science* **1998**, *281*, 2016−2018.
(12) Åkerman, M. E.; Chan, W. C. W.; Laakkonen, P.; Bathia, S. N.; Ruoslahti, E. *Proc. Natl. Acad. Sci. U.S.A.* **2002**, *99*, 12617−12621.
(13) Kim, S.; Bawendi, M. G. *J. Am. Chem. Soc.* **2003**, *125*, 14652−14653.
(14) Geissbuehler, I.; Hovius, R.; Martinez, K. L.; Adrian, M.; Thampi, K. R.; Vogel, H. *Angew. Chem.-Int. Ed.* **2005**, *44*, 1388−1392.
(15) Wu, X.; Liu, H.; Haley, K. N.; Treadway, J. A.; Larson, J. P.; Ge, N.; Peale, F.; Bruchez, M. P. *Nat. Biotechnol.* **2003**, *21*, 41−46.
(16) Pellegrino, T.; Manna, L.; Kudera, K.; Liedl, T.; Koktysh, D.; Rogach, A. L.; Keller, S.; Radler, J.; Natile, G.; Parak, W. P. *Nano Lett.* **2004**, *4*, 704−707.
(17) Luccardini, C.; Tribet, C.; Vial, F.; Marchi-Artzner, V.; Dahan, M. *Langmuir* **2006**, *22*, 2304−2310.
(18) Jin, T.; Fujii, F.; Sakata, H.; Tamura, M.; Kinjo, M. *Chem. Commun.* **2005**, 4300−4302.

10.1021/la061849h CCC: $33.50
Published on Web 10/07/2006

to make nanocrystal superlattice.[7] However, this method is limited to inorganic nanocrystals for which the conditions of nucleation preserve the organic template.

In the present paper, we demonstrate a simple method based on the solubilization of QD into a lyotropic phase to provide both types of materials (i.e., disperse nanoparticles or nanostructured materials). Our approach is to use an appropriate synthetic amphiphile to prepare self-ordered assembly of QD in water in a wide range of concentration, from a composite QD crystal liquid phase to isolated water-soluble QD micelles. The potential of lyotropic amphiphilic phases to form composite self-assembly of QD has not yet been investigated. Such nanostructured soft-materials can serve for the transport and the controlled release of drugs. For instance lyotropic phases presenting a lamellar or hexagonal DNA/lipidic structure were successfully used in gene therapy.[20,21] The potential of peptidic self-assembled mesophases have also been demonstrated for drug delivery.[22]

Experimental Section

Synthesis of QD. Two types of CdSe/ZnS QD, QD_{557} ($\lambda_{em} = 557$ nm in toluene, $Ø_{theoric}$=3.2 nm) and QD_{525} ($\lambda_{em} = 525$ nm in toluene, $Ø_{theoric}$=2.6 nm), were synthesized via pyrolysis of the organometallic precursors according to the literature.[9,23] Cadmium oxide CdO (0.051 g, Aldrich), trioctylphosphine oxide TOPO (3.77 g, 90% pure, Aldrich), tetradecylphosphonic acid (0.22 g, TDPA, Aldrich), and hexadecylamine (1.93 g, Aldrich) were mixed and heated at 340 °C under argon flow during 30 min on a Schlenk line. A selenium stock solution prepared from Selenium (0.116 g, Se, Alfa-Aesar) in trioctylphosphine (6.5 mL, TOP, Aldrich) was rapidly injected in the reaction mixture at 270 °C. The reaction was stopped after 5 min for QD_{525} and 11 min for QD_{557} by cooling the reaction vessel. CdSe QD cores were purified by precipitation in methanol/$CHCl_3$. Subsequently, a stock solution of Zn/S/TOP was prepared by mixing TOP (6 mL), diethylzinc in hexane (0.8 mL, Aldrich), and hexamethyldisilathiane (0.216 mL). To prepare the CdSe/ZnS QDs, the Zn/S/TOP stock solution was added to the CdSe QDs solution (at 5.13 mL/h) at 160 °C under vigorously stirring. After cooling at room temperature, the concentration of the resulting CdSe/ZnS QDs solution was then estimated from the optical density of the solution at 350 nm.[24] Commercial red QDs, QD_{605} ($\lambda_{em} = 600$ nm in toluene, $Ø_{theoric}$=4.6 nm, Quantum Dots Corporation, U.S.A.), were also used in this study.

Synthesis of Compound I. 3,4,5-Tris(*n*-dodecan-1-yloxy)benzoyl chloride (G12-COCl) was prepared from the corresponding acid[25] (G12-CO2H, 810 mg, 1.2 mmol) and oxalyl chloride (Aldrich, 5 mL). Poly(ethylene glycol) (PEG, $M_w = 1500$, Aldrich, 900 mg, 0.6 mmol), (dimethylamino)pyridine (DMAP, Aldrich, 150 mg, 1.23 mmol), and 1-ethyl-3-(3-(dimethylamino)-propyl) carbodiimide (EDC, Aldrich, 230 mg 1.2 mmol) were added and dissolved in 15 mL of dry CH_2Cl_2 with stirring. The reaction was allowed to proceed at room temperature for 20 h. The mixture was purified by 4 successive chromatographies (silica gel, eluent CH_2Cl_2/MeOH 95:5) to separate the diester (PEG-2G12) (392 mg, 24%) and the monoester **I** (255 mg, 20%). Anal. Calc. for **I** $C_{107}H_{206}O_{37}$, $2H_2O$ ($M_w = 2085$): C 60.60, H 9.98; C 60.23, H 10.31. ^{1}H NMR. **I**: 7.25 (s, 2H), 4.44 (t, 2H), 4.00 (t, 6H), 3.81 (t, 2H), 3.64 (m, 124H), 1.75 (m, 6H), 1.48 (m, 6H), 1.25 (m, 52H), 0.87 (t, 9H).

Quantum Dots Solubilization with I. CdSe/ZnS QDs were precipitated from initial TOPO/TOP stock solution with methanol, rinsed with methanol, and dried under vacuum. QDs were then redispersed in a dichloromethane solution of **I**, with a 1:2000 molar ratio of QD/**I**. After complete evaporation of dichloromethane, the dry film was hydrated with pure distillated water. After 2 h in a boiling water bath, the resulting solution was turbid and fluorescent under UV irradiation (at 365 nm). The solution was then centrifuged for 30 min at 15000*g* to remove aggregates and then ultracentrifuged at 100 000*g* for 30 min with a bed of 50% sucrose. The isolated QD micelles were then passed through a G25 spin column and dialyzed against water to eliminate sucrose. Finally, the solution of QD micelles (QD-**I)** was filtered through a 0.22 μm Millex GV filter.

Differential Scanning Calorimetry (DSC). The sample was introduced into an aluminum pan and submitted to several cycles of cooling and heating at 5 °C/min. Data are obtained from the second or third cycle. The measurements were performed on a Perkin-Elmer DSC7 instrument.

Small-Angle X-ray Scattering (SAXS). SAXS experiments were performed at the High Brilliance Beam Line (ID2) at European Synchrotron Radiation Facility (ESRF) in Grenoble, France. The undulator X-ray beam (wavelength 0.99 Å) was selected by a channel-cut Si(111) crystal and focused by rhodium-coated toroïdal mirror. The beam size defined by the collimated slits was 0.2 mm × 0.2 mm. The detector was an image-intensified charge-coupled device (CCD) camera. The sample-to-detector distance was 3.00 m. Samples were loaded in thin Lindman glass capillaries (diameter 1.0 ± 0.1 mm and thickness 10 μm; GLAS, Muller, Berlin, Germany) sealed with wax. Concerning QD/**I** samples, QD and **I** (1:21 000) were solubilized in dichloromethane. After complete evaporation of the solvent, the residue was introduced in capillary and 200 μL of water was added and left to diffuse into the residue. The high flux led us to decrease the acquisition time to 300 ms. All samples exhibited powder diffraction, and the scattering intensities as a function of the radial wave vector were determined by circular integration.[26]

Electron Density Reconstruction of the Hexagonal Phase. The electronic density $\rho(r)$ was reconstructed perpendicularly to the water channel applying the following formula[27,28] on the observed diffraction peaks

$$\rho(r) \propto \sum_{n=1,3,4,7} F_n J_0\left(2\pi r \frac{2\sqrt{n}}{\sqrt{3}a}\right)$$

where F_n is the structural factor related to the square root of peak intensity, n is the Bragg reflection order, J_0 is the 0 order of Bessel function, r is the radial distance from the center of the column, and a is the lattice parameter of the hexagonal structure. The electronic density of the identified hexagonal phase was reconstructed with four peaks in the diffraction pattern ($n = 1$, 3, 4, and 7). Simple molecular assumptions on the electronic density profiles in the phase[29] allow us to exclude false solutions. These criteria are (1) QD nanocrystals have the highest electronic density, (2) followed by the gallate central group, and (3) the electron density decrease regularly along the alkyl chains up to a minimum corresponding to the terminal methyl.

Dynamic Light Scattering (DLS). DLS measurements were performed at a scattering angle of 90° at 25 °C on Zetasizer ZEN3600 (Malvern Instruments, England). All solutions were previously filtered through 0.2 μm Millipore filter (Millex GV, Sigma-Aldrich, France).

Transmission Electron Microscopy (TEM). A total of 4 μL of the sample was deposited from a dilute solution on a 3−4 nm thick

(19) Lee, S. W.; Mao, C.; Flynn, C. E.; Belcher, A. M. *Science* **2002**, *296*, 892−895.
(20) Rädler, J. O.; Koltover, I.; Salditt, T.; Safinya, C. R. *Science* **1997**, *275*, 810−814.
(21) Artzner, F.; Zantl, R.; Rapp, G.; Rädler, J. *Phys. Rev. Lett.* **1998**, *81*, 5015−5018.
(22) Valéry, C.; Paternostre, M.; Robert, B.; Gulik-Krzywicki, T.; Narayanan, T.; Dedieu, J.-C.; Keller, G.; Torres, M.-L.; Cherif-Cheikh, R.; Calvo, P.; Artzner, F. *Proc. Natl. Acad. Sci. U.S.A.* **2003**, *100*, 10258−10262.
(23) Peng, X.; Schlamp, M. C.; Kadavanich, A. V.; Alivisatos, A. P. *J. Am. Chem. Soc* **1997**, *119*, 7019.
(24) Qu, L.; Peng, X. *J. Am. Chem. Soc.* **2002**, *124*, 2049.
(25) Percec, V.; Ahn, C.-H.; Bera, T.; Ungar, G.; Yeardley, D. J. P. *Chem.−Eur. J.* **1999**, *5*, 1070−1083.
(26) Narayanan, T.; Diat, O.; Bösecke, P. *Nucl. Instrum. Methods Phys. Res. A* **2001**, *465−468*, 1005−1009.
(27) Tardieu, A.; Luzzati, V.; Reman, F. C. *J. Mol. Biol.* **1973**, *75*, 711−733.
(28) Hauet, N.; Artzner, F.; Boucher, F.; Grabielle-Madelmont, C.; Cloutier, I.; Keller, G.; Lesieur, P.; Durand, D.; Paternostre, M. *Biophys. J.* **2003**, *84*, 3123−3137.
(29) Harper, P. E.; Mannock, D. A.; Lewis, R. N. A. H.; McElhaney, R. N.; Gruner, S. M. *Biophys. J.* **2001**, *81*, 2693−2706.

film of amorphous carbon supported on a 300 mesh copper grid (Oxford Instruments, G2300C, England), and the solvent was blotted with a filter paper. The grids were observed in a Philips CM 12 at an accelerating voltage of 10 kV. Images were recorded on Kodak S.O 163 film under low dose conditions at 22 000× magnifications and ~2.3 μm underfocused. The micrographs were digitized at 1200 dpi with the UPRES-A 6026 scanner. The size distributions of the nanocrystal samples were estimated by analyzing the scanned TEM negatives with Imaq vision builder (version 6.1, National Instruments, USA).

Optical Properties of QD. Absorbance measurements of QD solution were performed by a Cary 100 UV−visible scan spectrophotometer (Varian, Australia). Fluorescence spectra were measured by LPS Quanta-Master (Photon Technology International, England). Moreover to calculate the quantum yield (QY) of QDs before and after functionalization, spectrally integrated emission of nanocrystals were compared to the emission of rhodamine 6G in ethanol at identical optical density of 0.015, using the formula from literature.[30]

Preparation of Giant Unilamellar Vesicles (GUVs). GUVs were obtained with the electric swelling method.[31] GUVs were prepared in a chloroform/methanol mixture 9:1 v/v at 95% egg phosphatidylcholine (EPC, Sigma-Aldrich, France) and 5% *N*-[1-(2,3-dioleoyloxy)propyl]-*N*,*N*,*N*-trimethylammonium chloride (DOTAP, Sigma-Aldrich, France) in molar mass.

Dark Field, Polarized Light Optical, and Fluorescence Microscopy. QD-**I** in contact with GUVs were observed either by dark field or by epifluorescence on an inverted microscope IX71 (Olympus, Japan) equipped with a 40× objective (Olympus, Japan). QD were excited at 365 nm by a high vacuum mercury lamp. Images were acquired by a camera colorview II, Soft Imaging system (Olympus, Japan). To observe the textures of lyotropic phases of **I** at 50 °C, a droplet of **I** was putted into contact with pure water.

High-Pressure Liquid Chromatography (HPLC). HPLC, based on size exclusion of QD-**I** solution, was performed on a Waters HPLC system on a Superdex 200 GL column (10 × 300, 13 μm, Amersham Biosciences, France) using a phosphate buffer saline mobile phase (0.01 M phosphate buffer, 0.0027 M KCl, 0.137 M NaCl, pH 7.4) at a flow rate of 0.5 mL/min. Absorbance detections were performed online during the separation.

Results and Discussion

Synthesis and Self-Organization of I. Due to their ability to self-assemble into different highly curved phases,[32−35] we used pegylated gallate amphiphiles to disperse the QD in water. In comparison to phospholipids,[3,14] gallate molecules are easily synthesized, and small changes in their molecular structure strongly affect the morphology of their lyotropic phase. An amphiphile, named **I**, was designed from an aromatic core (gallate) grafted with three dodecyl chains for inducing a strong hydrophobic interaction with the TOPO ligand of the surface (Scheme 1, a and b). As polar a headgroup, a poly(ethylene glycol) chain (PEG, 1500 in molar mass) was introduced to stabilize functionalized nanocrystals against flocculation under physiological conditions or strong ionic strength[36] and to prevent nonspecific adsorption.[37,38] The length of the PEG group was chosen to adjust the hydrophilic/hydrophobic balance of the molecule and to avoid the formation of inverted curved phases.

Scheme 1. (a) Chemical Structure and Schematic Representation of I (b) Schematic Representation of Functionalized QD by I

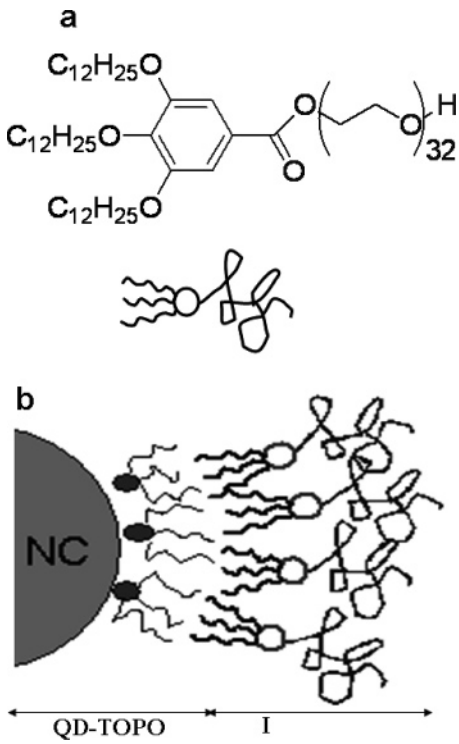

[In the case of a short PEG chain (PEG, 370 in molar mass), an inverted hexagonal phase was observed in which QDs are completely insoluble.] The synthesis of **I** was carried out first by the trialkylation of the gallic methyl ester followed by its saponification. The obtained acid was then condensed with commercial PEG.

To determine the self-organization of the compound **I** alone, the temperature of the phase transitions for pure **I** and for a **I**/water mixture with a 1:1 mass ratio were determined by DSC (Supporting Information, Table A). For the pure compound, the transition observed around 40 °C was attributed to the fusion of the dodecyl chains. By cooling, a supercooling was observed before the recrystallization of the dodecyl chains at 25 °C. In the presence of water, the position of the phase transition was decreased to 10 °C either by heating or cooling attributed to the fusion of the chains. To identify the lyotropic phases of **I**, SAXS experiments were performed at 50 °C to avoid the crystalline form. In the presence of pure water, **I** reveals a rich polymorphism (Figure 1a). Following the increase in water content, **I** successively adopts a lamellar phase with a characteristic parameter $a = 82$ Å, a cubic phase *Ia3d* with $a = 269$ Å, and finally a direct hexagonal phase with $a = 120-134$ Å. Typical textures of lamellar (Figure 1d) and hexagonal phases (Figure 1c) were also observed by optical light polarized microscopy in the contact zone between pure **I** and water. For higher water content, a broad peak attributed to micelles was observed by SAXS. The presence of the micelles was confirmed by DLS measurements on a solution of **I** (2.9×10^{-6} M) which revealed the presence of two populations with a mean hydrodynamic diameter at 102 and 24 nm (Supporting Information, Table B). When imaged by TEM after phosphotungstic acid staining (Figure 1b), this solution showed the presence of columnar aggregates that could explain the polydispersity of the population. The phosphotungstic acid

(30) Lackowicz, J. R. *Principles of Fluorescence Spectroscopy*, 2nd ed.; Kluwer Academic: New York, 1999.
(31) Marchi-Artzner, V.; Gulik-Krzywicki, T.; Guedeau-Boudeville, M.-A.; Gosse, C.; Sanderson, J. M.; Dedieu, J.-C.; Lehn, J.-M. *ChemPhysChem* **2001**, *2*, 367−376.
(32) Percec, V.; Heck, J. A.; Tomazos, D.; Ungar, G. *J. Chem. Soc., Perkin Trans.* **1993**, *2*, 2381−2388.
(33) Percec, V.; Cho, W.-D.; Ungar, G.; Yeardley, D. J. P. *Chem.—Eur. J.* **2002**, *8*, 2011−2025.
(34) Kishikawa, K.; Furusawa, S.; Yamaki, T.; Kohmoto, S.; Yamamoto, M.; Yamaguchi, K. *J. Am. Chem. Soc.* **2002**, *124*, 1597−1603.
(35) Fuchs, P.; Tschierske, C.; Raith, K.; Das, K.; Diele, S. *Angew. Chem., Int. Ed.* **2002**, *41*, 628−631.
(36) Wind, B.; Killmann, E. *Colloid Polym. Sci.* **1998**, *276*, 903−912.
(37) Jones, M. C.; Leroux, J. C. *Eur. J. Pharmacol. Biopharm.* **1999**, *48*, 101−111
(38) Torchilin, V. P. *Adv. Drug Delivery Rev.* **2002**, *54*, 235−252

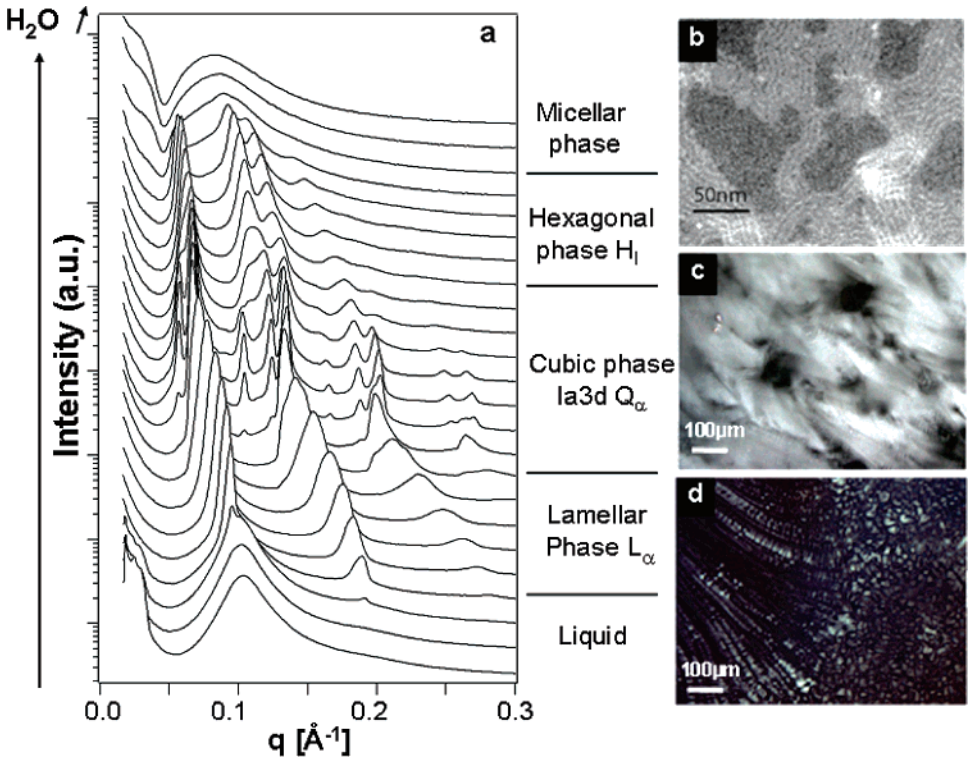

Figure 1. (a) SAXS spectra of **I** in contact with water gradient, at 50 °C. (b) TEM images of **I** in solution (6 mg/mL) stained by phosphotungstic acid (2%, pH 7). Polarized optical microscopy images of **I** in contact with water at 50 °C (c) in hexagonal phase and (d) in lamellar phase.

stained only the hydrophilic part of the molecule which corresponds to dark areas on the TEM image. The white hydrophobic fibers with a diameter of 7 nm are oriented parallel with an inter distance of 3 nm imposed by the steric hindrance of the PEG chains. This distance (corresponding to $2R_g$) is in agreement with the radius of gyration R_g of PEG (1500 in molar mass) estimated to be about 1.4 nm according to the literature.[39] Similar fibrous self-assemblies of pegylated lipids have previously been observed.[40]

Composite Hexagonal Phase of QD/I. We next tested the incorporation of nanocrystals in the lyotropic phase of **I**. We used homemade CdSe/ZnS QD, designated as QD_{557} (peak emission λ_{em}= 557 nm in toluene) and QD_{525} and synthesized according to the literature,[9,23] as well as commercial QD_{605} (λ_{em}= 605 nm in toluene, Quantum Dot Corporation, U.S.A.). QD/**I** mixtures were first observed by polarized optical microscopy and fluorescence microscopy at around 50 °C. In the presence of QDs, textures of hexagonal phases (conic focal) and lamellar (oily streaks) were observed on pure **I** in the presence of water as shown respectively in Figure 2, panels a and c. In the case of the hexagonal phases, the fluorescence appears homogeneously distributed within the textures (Figure 2b), whereas only fluorescent aggregates are visible in the case of the lamellar phase (Figure 2d). Interestingly, after the insertion of QD, the hexagonal phase remains stable after cooling at room temperature, preventing the crystalline form of **I**.

To confirm the insertion of QDs into the hexagonal phase, the structure of pure **I** and hybrid QD/**I** self-assembly was analyzed by SAXS. Typical trace of pure **I** is shown in Figure 2e. The attribution of the different peaks reveals the formation of a direct hexagonal phase with a lattice parameter a equal to 162 Å superposed to the signal of micelles. At the same temperature, a QD/**I** mixture (molar ratio 1:21000) in the presence of water exhibited a hexagonal phase with a = 137 Å (Figure 2e). This parameter is independent of the water concentration, excluding a dilatation of the hydrophilic PEG part with the water concentration (Supporting Information, Figure A).

The difference in electronic densities between pure **I** and the QD/**I** mixture allowed the localization of QD within the hexagonal phase to be precisely determined. From the diffraction peak intensities represented in Figure 2e, the radial electronic density profile was calculated and represented on a distance equal to a/2. For pure **I**, the maximum of electronic density located at 30 Å was attributed to the gallate part of the amphiphile (Figure 3a). For the QD/**I** mixture, a larger maximum, located at the origin of the hydrophobic core of hexagonal phases, can be attributed to the inorganic nanocrystals (Figure 3b). Therefore, the distribution in electronic density is in agreement with the inclusion of QD in the hydrophobic core of the hexagonal columns.

In the case of pure **I**, the broadness of the peak centered around 30 Å indicates a relative disorder in the radial distribution of molecules. In this case, the hexagonal phase parameter is imposed by the molecular area of PEG headgroups, and the alkyls chains are too short to fill up the hydrophobic core of the column creating a so-called frustrated phase. Then, the inclusion of QD within the hydrophobic core compensates this frustration and results in a more ordered phase with a smaller a parameter. These results show that it is possible to form a hybrid inorganic−organic self-assembly of QD/**I** organized in a hexagonal columnar phase.

Isolated Pegylated Micelles of QD-I. Since the molecule **I** forms micelles in a diluted regime, the question arises of whether the hybrid hexagonal QD phase can be converted into isolated QD micelles. To evaluate this possibility, the hydration of a dried QD/**I** (1:2000) mixture was performed under diluted conditions at 60 °C. The resulting suspension, initially turbid, was successively ultra-centrifuged (100 000*g* for 45 min onto a

(39) Kawagushi, S.; Imai, G.; Susuki, J.; Miyahara, A.; Kitano, T. *Polymer* **1997**, *38*, 2885.

(40) Takeoka, S.; Mori, K.; Ohkawa, H.; Sou, K.; Tsuchida, E. *J. Am. Chem. Soc.* **2000**, *122*, 7927−7935.

(41) Michalet, X.; Pinaud, F. F.; Bentolila, L. A.; Tsay, J. M.; Doose, S.; Li, J. J.; Sundaresan, G.; Wu, A. M.; Gambhir, S. S.; Weiss, S. *Science* **2005**, *307*, 538−544.

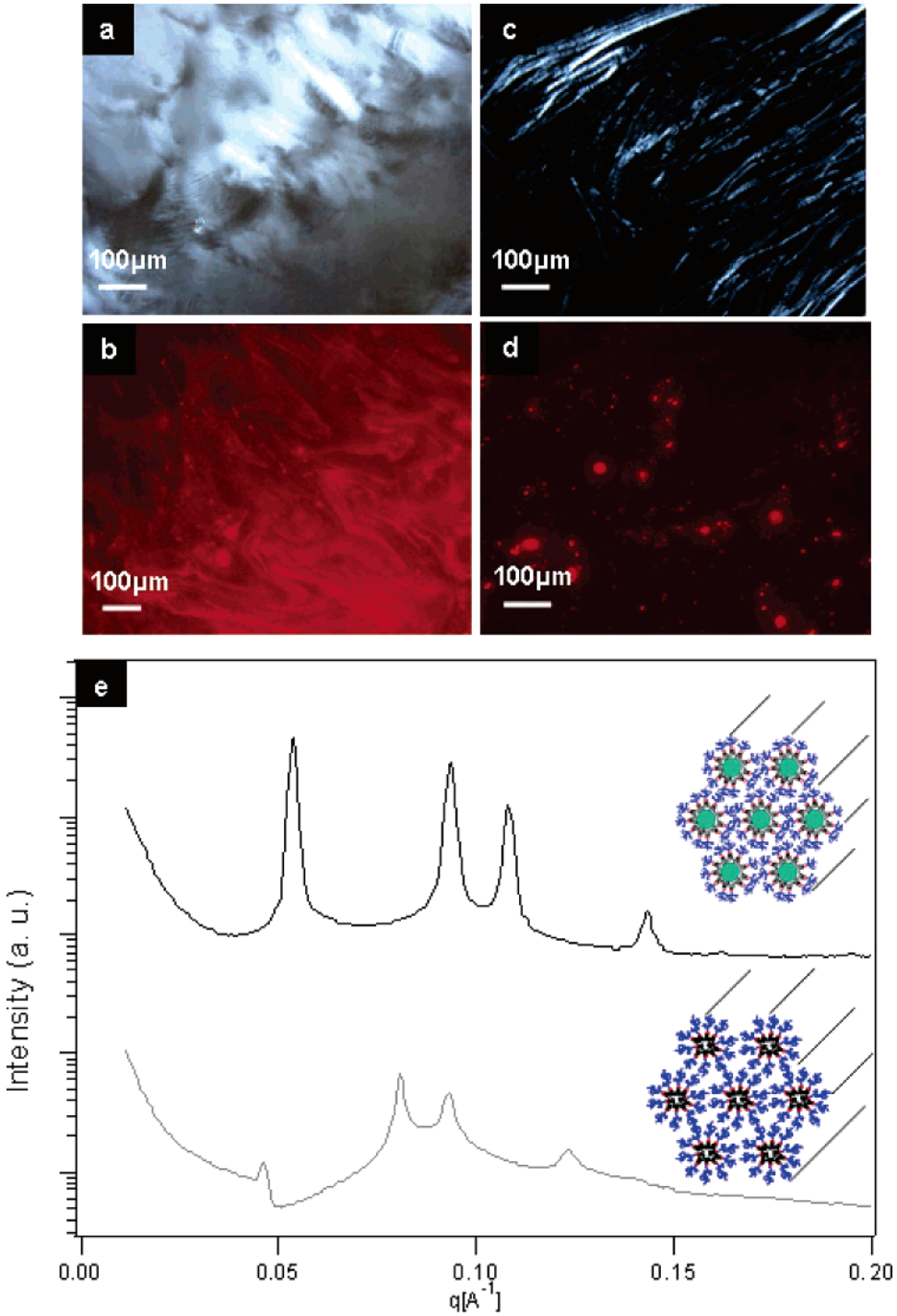

Figure 2. Optical microscopy images of QD_{605}/**I** mixtures in contact with water at 50 °C. Observation in polarized mode and in fluorescence mode (a and b) of hexagonal phase and (c and d) of lamellar phase. (e) SAXS pattern at 20 °C (gray line) of pure **I** and (black line) of QD_{557}/**I** mixture (1:21000) at low water content adopting hexagonal phases and their respective schematic representation. The green part represents the zone occupied by the QD.

cushion of 50% sucrose), dialyzed against water, and filtrated to produce an optically clear fluorescent solution. Before centrifugation, the size distribution measured by DLS of the micelles presents two peaks (Supporting Information, Table B). The first one has a hydrodynamic diameter D_h equal to 130−190 nm and corresponds to columnar aggregates already observed by TEM for pure **I** (Figure 1b). The second peak, $D_h \sim 25$ nm, is related to micelles. A similar micellization process was demonstrated in the case of a PEG−phospholipids and QD mixture where QD micelles were obtained by dilution into water.[3] Here the contribution of the micelles in the scattered intensity was increased by the presence of QD, maybe due to an increase in number of scattering objects or a change in refractive index due to the insertion of the QD. Interestingly, D_h of encapsulated QD-**I** appears similar to that observed for micelles of pure **I**. As previously discussed in the case of QD/**I** hybrid hexagonal phase (low water content), nanocrystals have probably a stabilizing effect by providing a template for an ordered distribution of amphiphiles, and as a result they facilitate the formation of small micelles. After elimination of the columnar aggregates by ultracentrifugation, DLS measurements yielded value of D_h, in the range 20−35 nm (Table 1).

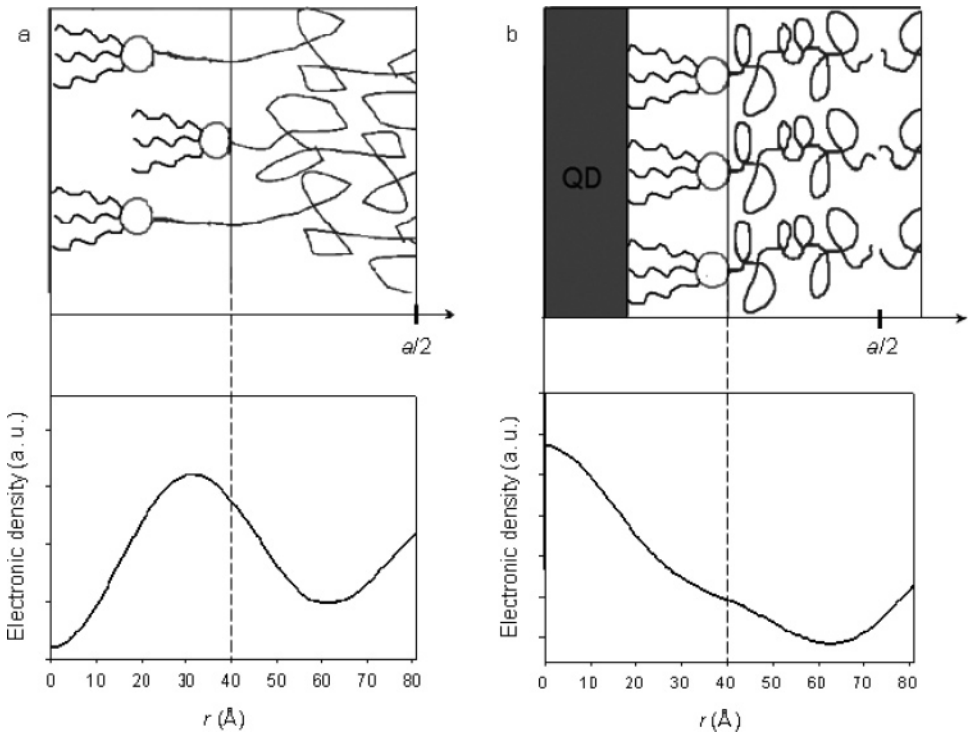

Figure 3. Radial electronic density profile of (a) pure **I** and (b) QD_{557}/**I** mixture in hexagonal phase and their respective schematic view of the possible organization along *r*, radial distance. Radial electronic densities were calculated from the intensity of diffraction peaks represented in Figure 2e (method of calculation in the Experimental Section).

Table 1. Hydrodynamic Diameter D_h (Mean ± Standard Deviation (SD)) and Scattered Intensity *I* Obtained by DLS and Inorganic Diameter d_{QD} (Mean ± Standard Deviation (SD)) of QD-I Suspensions after Isolation by Ultracentrifugation[a]

type of QD	d_{QD} ± SD (nm)	D_h ± SD (nm)	*I* (%)
QD_{525}-**I**	3.7 ± 1.5	24 ± 9	94
QD_{557}-**I**	3.9 ± 1.6	19 ± 4	97
QD_{605}-**I**	4.5 ± 1.5	34 ± 12	90

[a] d_{QD} corresponds to the inorganic core−shell of the functionalized nanocrystals and was estimated from TEM images.

To further purify the QD-**I** micelles, functionalized QD-**I** suspension and a micellar solution of pure **I** were chromatographied through a size exclusion column using HPLC. QD_{605}-**I** suspension yields two main peaks (revealed by UV absorption at 254 nm) with elution times of 16.1 and 18 min (Figure 4a). The first one presents a fluorescence emission at 605 nm and corresponds to the isolated QD-**I** (Figure 4b). The second one (at 18 min) is attributed to free micelles, as confirmed by comparison of UV spectra to **I** micelles solution (Figure 4b, insert).

All of the samples were imaged by TEM to observe the inorganic (electron-dense) core/shell of QD. As shown in Figure 5a for QD_{525}-**I**, all prepared QD-**I** micelles appear as isolated. No large aggregates were observed. The inorganic diameter (mean ± SD) of QD_{557}-**I**, QD_{525}-**I**, and QD_{605}-**I** were respectively 3.9 ± 1.6 (sample size = 603), 3.7 ± 1.5 (sample size = 838), and 4.5 ± 1.5 nm (sample size = 958) in agreement with the expected value from their emission wavelength[24] (Figure 5b and Table 1).

Optical Properties of QD-I. Optical properties of QD-**I** were analyzed by absorption and fluorescence spectroscopy. The emission spectra of QD, recorded before and after the functionalization, showed a small red-shift (∼5 nm) in the peak emission. This red-shifting effect has already been noticed for peptide coating[10] and has been attributed to the hydrophobic domain of peptide ligand in close contact with QD surface. The full width at half maximum (fwhm) of the emission spectra (30

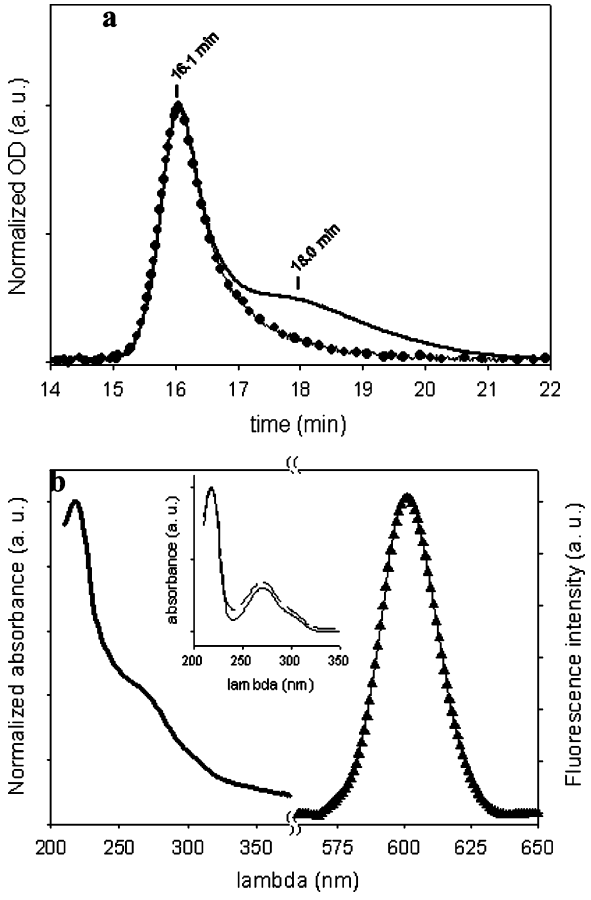

Figure 4. (a) HPLC spectra of QD_{605}-**I** suspension measured by UV detection (—) at 254 nm and (●) at 350 nm, (b) (—) UV and (▲) fluorescence spectra of QD_{605}-**I** fraction withdrawn at elution time of 16.1 min, in the insert UV spectra of (—) **I** solution and (− −) QD_{605}-**I** fraction withdrawn at elution time of 18 min.

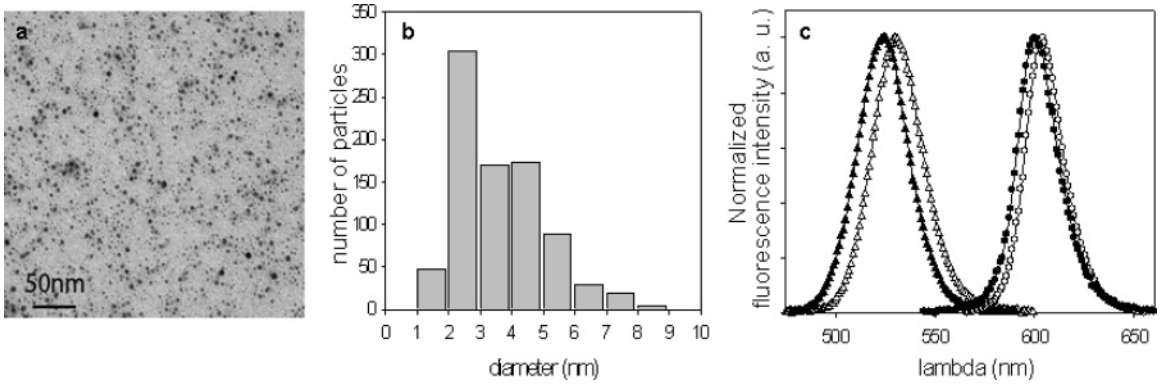

Figure 5. (a) TEM images of QD_{525}-**I** solubilized in water and (b) its size distribution with average diameter: 3.7 ± 1.5 nm. (c) Normalized fluorescence intensity, obtained at 350 nm excitation wavelength, of (▲) QD_{525} solubilized in chloroform before functionalization (emission peak at 525 nm), (△) QD_{525}-**I** solubilized in water (emission peak at 530 nm), (●) QD_{605} solubilized in chloroform before functionalization (emission peak at 600 nm) and (○) QD_{605}-**I** solubilized in water (emission peak at 604 nm).

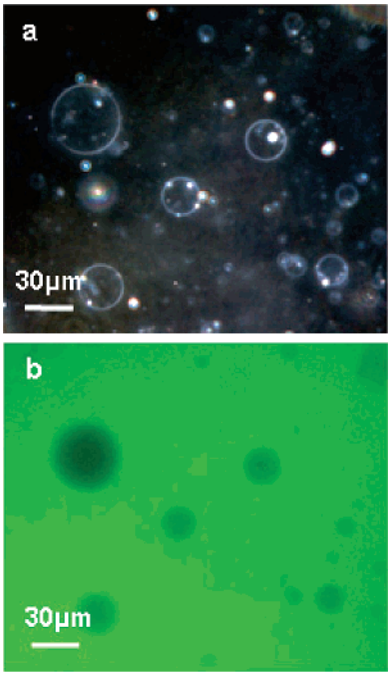

Figure 6. QD_{525}-**I** and GUVs interactions observed by (a) dark field and (b) fluorescence optical microscopy images.

nm for QD_{525} and 24 nm for QD_{605}) was not modified, showing that the functionalization process does not alter the size distribution. Finally, we determined the quantum yield (QY) of nonfunctionalized and functionalized QD_{525}-**I** using rhodamine 6G in ethanol as a standard.[30] The QY of TOPO-coated QD_{525} in chloroform was $16 \pm 4\%$, very similar to the value of QD_{525}/**I** micelles in water ($24 \pm 6\%$). Altogether, these observations show that the fluorescence properties of the QD are preserved after coating by the amphiphilic molecule.

Interactions of QD-I with Lipidic Membranes. To further establish the potential of QD/**I** micelles as fluorescent biolabels, we tested their nonspecific binding of nanocrystals to lipidic or cell membranes by optical fluorescence microscopy. For this purpose, we prepared giant unilamellar vesicles (GUV) according to the literature[31] and visualized them by dark field optical microscopy (Figure 6a). A nanomolar solution of QD_{525}-**I** was incubated for 1 h in the presence of GUV. The fluorescence of QD_{525}-**I** was homogeneously distributed in the solution, and GUV appeared as a black area clearly showing that there is no adsorption of QD onto the lipidic membranes (Figure 6a,b). As a control, a nanomolar solution of negatively charged QD_{525} coated with 11-mercapto undecanoic acid (QD_{525}-MUA) was incubated in the presence of positively charged giant vesicles. A strong adsorption of the QDs onto the vesicle membrane was observed by fluorescence microscopy (see Figure B in the Supporting Information). In addition, we checked the interaction of QD_{525}-**I** micelles with cultured Hela cells. After 10-mn incubation of a nanomolar solution of QDs followed by repetitive washing, we did not observe any fluorescent signal, further indicating that the presence of PEG prevents the nonspecific adsorption of QDs onto membranes.

Conclusion

In conclusion, the use of the amphiphile molecule **I**, presenting a rich polymorphism, enabled the preparation of a composite inorganic−organic QD mesophase in water. A direct hybrid hexagonal phase was obtained by simple hydration of a QD/**I** mixture. Indeed, polarized optical microscopy and SAXS results have confirmed the inclusion of QD in hydrophobic core of the columnar phase leading to a more ordered phase. Such self-ordered mesophase offers the possibility to encapsulate and then transport different types of inorganic nanocrystals. In addition, the morphology of such composite phase can be changed by water concentration and have therefore potential application in the controlled release of functional nanoparticles. By simple dilution in water, this mesophase can be converted into isolated water-soluble QD-**I** micelles with a diameter of around 25 nm. The presence of PEG at the surface of QD-**I** micelles efficiently prevents the nonspecific adsorption of QD onto lipidic and cellular membranes. In addition, the pegylated amphiphile **I** could be chemically modified to introduce a specific targeting recognition group at the polar headgroup. Therefore, the present method offers the possibility to prepare either functional fluorescent nanoprobes or composite mesophase opening the route to the fabrication of new bioactive functional materials.

Acknowledgment. The work was supported by ACI DRAB, ANR PNANO, and Région Bretagne, especially for financial support of F.B. We are thankful to Prof. C. Ricolleau (Université Paris 7, France) for fruitful discussions about TEM. European Synchrotron Radiation (Grenoble, France) Facility is acknowledged for provision of beam time.

Supporting Information Available: Temperature and enthalpy of fusion data for pure **I** (Table A). D_h and scattered intensity distribution data for **I** (Table B). SAXS spectra of a QD_{557}/**I** mixture (Figure A). Fluorescence microscopy image of QD_{525}-MUA coated with 11-mercapto undecanoic acid (Figure B). This material is available free of charge via the Internet at http://pubs.acs.org.

LA061849H